Sum frequency generation and solid-state NMR study of the structure, orientation, and dynamics of polystyrene-adsorbed peptides

Tobias Weidner[a], Nicholas F. Breen[b], Kun Li[b,c], Gary P. Drobny[b,c], and David G. Castner[a,d,1]

[a]Department of Bioengineering and National ESCA and Surface Analysis Center for Biomedical Problems, University of Washington, Seattle, WA 98195; [b]Department of Chemistry, University of Washington, Seattle, WA 98195; [c]Department of Physics, University of Washington, Seattle, WA 98195; and [d]Department of Chemical Engineering, University of Washington, Seattle, WA 98195

Edited by Gabor A. Somorjai, University of California, Berkeley, CA, and approved May 24, 2010 (received for review March 22, 2010)

The power of combining sum frequency generation (SFG) vibrational spectroscopy and solid-state nuclear magnetic resonance (ssNMR) spectroscopy to quantify, with site specificity and atomic resolution, the orientation and dynamics of side chains in synthetic model peptides adsorbed onto polystyrene (PS) surfaces is demonstrated in this study. Although isotopic labeling has long been used in ssNMR studies to site-specifically probe the structure and dynamics of biomolecules, the potential of SFG to probe side chain orientation in isotopically labeled surface-adsorbed peptides and proteins remains largely unexplored. The 14 amino acid leucine-lysine peptide studied in this work is known to form an α-helical secondary structure at liquid-solid interfaces. Selective, individual deuteration of the isopropyl group in each leucine residue was used to probe the orientation and dynamics of each individual leucine side chain of LKα14 adsorbed onto PS. The selective isotopic labeling methods allowed SFG analysis to determine the orientations of individual side chains in adsorbed peptides. Side chain dynamics were obtained by fitting the deuterium ssNMR line shape to specific motional models. Through the combined use of SFG and ssNMR, the dynamic trends observed for individual side chains by ssNMR have been correlated with side chain orientation relative to the PS surface as determined by SFG. This combination provides a more complete and quantitative picture of the structure, orientation, and dynamics of these surface-adsorbed peptides than could be obtained if either technique were used separately.

protein | surface | isotope labels | solid-liquid interface

Controlled immobilization of peptides onto artificial biointerfaces plays a key role in developing antifouling, implant, and immunosensor technologies. Development of biocompatible surfaces is also a major focus of the materials and tissue engineering communities (1–4), particularly for using peptide or protein coatings in recreating a natural extracellular matrix to direct wound repair or tissue development and homeostasis (5–7). Understanding the structural and dynamic impact of protein adsorption at the molecular level is therefore crucial for the design of future bioactive surface coatings and interfaces.

Sum frequency generation (SFG) spectroscopy has proven to be an increasingly powerful technique for probing protein films in situ at the solid-liquid interface (8–16). According to the "selection rules" of SFG, only molecular groups in proteins or peptides at an interface that have a net order will contribute to the measured signal (17). Since surface interactions can introduce ordering in the binding regions of proteins and peptides, SFG is an excellent probe to identify the side chains involved in these binding events (9–11, 15) and, in some cases, the orientation of adsorbed peptides (18). Backbone related amide modes, which are sensitive to conformation (19), can also determine the secondary structure of adsorbed peptides (14, 20, 21).

Solid-state nuclear magnetic resonance (ssNMR) is likewise a versatile probe of biomolecular structure. In recent years, multidimensional ssNMR experiments incorporating dipolar recoupling pulse sequences have led to high resolution structures of proteins in micro-crystalline form (22, 23). Recently, ssNMR techniques have been used to obtain structural parameters such as internuclear distances and bond torsion angles for the biomineralization protein salivary statherin adsorbed onto hydroxyapatite crystal surfaces (24–27), which combined with the protein structure prediction algorithm RosettaSurface (28) have produced an atomic level structural model (29).

In addition to structural information, deuterium ssNMR (^{2}H NMR) line shapes and relaxation can probe the amplitudes and rates of local internal motions of proteins and nucleic acids for rates ranging from 10^{12} Hz to less than 10^4 Hz. ^{2}H NMR has long been used to determine the degree to which amino acid side chain dynamics are sensitive to structural environment, for example, the perturbation of the motion of leucine side chains in collagen fibrils (30), the dynamic impact of polylysine adsorption onto silica and hydroxyapatite surfaces (31), and the dynamics of hydrophobic side chains in membrane-associated proteins (32–34). Additionally, ^{13}C-^{2}H NMR correlation techniques have been used by Reif and coworkers to identify the dynamics of deuterated valine and leucine side chains in uniformly ^{13}C-labeled micro-crystalline proteins (35, 36).

The question arises, can the orientation or proximity of protein side chains relative to the surface as determined by SFG, be correlated with trends in the dynamics of the same protein side chains as determined by ssNMR? Recent ssNMR studies of statherin and amelogenin show that proximities of protein side chains to surfaces can be directly detected by rotational echo double resonance (REDOR) recoupling, if the surface contains a NMR-active nucleus such as ^{31}P or ^{19}F that is not also ubiquitous in the protein (24, 37, 38). In the absence of an NMR-active nucleus located exclusively in the surface, protein interactions with charged surfaces can be detected as perturbations of the ^{13}C chemical shift of certain side chain functional groups, such as carboxyls (27).

But in the absence of circumstances that enable quantitative determination of protein side-chain-surface distances by dipolar recoupling, or qualitative description from chemical shift perturbations, no simple NMR means exists to determine protein side-chain-surface proximities. In such cases, correlating dynamic NMR data with side-chain–surface proximities determined by SFG is a viable alternative, but only if SFG signals are acquired site specifically.

To demonstrate this combined spectroscopic approach, we use synthetic "LK" model peptides, first demonstrated by DeGrado

Author contributions: G.P.D. and D.G.C. designed research; T.W. and N.F.B. performed research; T.W., N.F.B., and K.L. analyzed data; and T.W., N.F.B., G.P.D., and D.G.C. wrote the paper.

The authors declare no conflict of interest.

This article is a PNAS Direct Submission.

[1]To whom correspondence should be addressed. E-mail: castner@nb.uw.edu.

This article contains supporting information online at www.pnas.org/lookup/suppl/doi:10.1073/pnas.1003832107/-/DCSupplemental.

and Lear to adopt particular structures and orientations at interfaces (39), consisting of alternating periods of leucine (L) and lysine (K) residues (Fig. 1*A*). Previously, we used dipolar recoupling and double-quantum NMR techniques to quantify the α-helical structure secondary structure of a 14-residue peptide, LKα14: Ac-LKKLLKLLKKLLKL-OH adsorbed onto polystyrene (PS) surfaces (40).

The structure and orientation of LKα14 on PS and silica surfaces has been studied by Somorjai and coworkers (10, 13) using SFG vibrational spectroscopy. We have also studied the structure and orientation of LKα14 on PS, silica, self-assembled monolayers (SAMs), and fluorocarbon (FC) surfaces using SFG combined with other spectroscopic methods (9, 16, 18, 41–43). These studies show that adsorbed LKα14 has an α-helical secondary structure, and on the hydrophobic surfaces (PS and FC) the leucine side chains were oriented towards, and the lysine side chains oriented away from, the surface. Recent SFG studies using SAMs on gold have provided definitive proof that the leucine side chains orient towards hydrophobic surfaces (18). However, the orientations of *individual* side chains were not previously determined. In the present study we use selective deuteration to show that SFG can quantify the individual surface orientation of each of the eight leucines in LKα14 adsorbed onto PS and these orientations can be correlated with trends in ^{2}H NMR-derived dynamics obtained from the same adsorbed peptides. In *Procedures* we will briefly describe SFG and ^{2}H NMR methods only as they apply to the specific case of leucine side chains interacting with a hydrophobic surface. After outlining the materials and methods used and a presentation of the results, we will discuss correlations of the SFG and NMR data and prospects for future SFG/NMR studies of more complicated surface-adsorbed peptides/proteins.

Procedures

Sum Frequency Generation. SFG is a coherent nonlinear optical process where spectrally tunable infrared and fixed visible laser pulses are overlapped in time and space at an interface and generate photons at the sum of the pump beam frequencies. The intensity of the generated SF light I_{SF} is given by:

$$I_{SF} \propto |\chi^{(2)}_{eff}|^2 I_{IR} I_{vis} \quad [1]$$

here, I_{vis} and I_{IR} are the infrared and visible pump beam intensities, respectively, and $\chi^{(2)}_{eff}$ denotes the effective second-order nonlinear susceptibility of the interface which can be written as (44):

$$I_{SF} \propto |\chi^{(2)}_{eff}|^2 = \left|\chi^{(2)}_{NR} + \sum_{\nu} \frac{A_\nu e^{i\phi_\nu}}{\omega_{IR} - \omega_\nu + i\Gamma_\nu}\right|^2. \quad [2]$$

Here, $\chi^{(2)}_{NR}$ is the second-order nonlinear susceptibility of the nonresonant background, A_ν is the strength of the νth vibrational mode, ϕ_ν denotes the phase of the respective mode and ω_{IR} refers to the frequency of the incident IR field. ω_ν and Γ_ν are the resonance position and width of the respective modes. Fitting **[2]** to the spectral data allows us to determine A_ν, ω_ν, and Γ_ν.

By varying the *s* or *p* polarization of the pump beams and the detected SFG signal, it is possible to probe different elements of the $\chi^{(2)}$ tensor. For example, *ssp* polarization denotes *s* polarized sum, *s* polarized visible and *p* polarized IR light. In this study *ssp*, *ppp*, and *sps* combinations were used. The resonance strengths for the different polarization combinations can be related to molecular susceptibilities of SFG active groups in laboratory coordinates using procedures established by Shen and coworkers (45).

For the orientation analysis of the leucine side chains we used the united atom approach first employed by Cremer and coworkers (46). Briefly, instead of treating the vibrational modes of the two terminal methyl groups individually, the hyperpolarizabilities of the isopropyl moiety are combined in the molecular structure. The advantage of transforming from a methyl-based structure to an isopropyl-based structure is the 2× reduction of coordinates (six for the two individual methyls to three for the unified system) required to define the position of the isopropyl group. Fig. 1*B* illustrates the unified coordinates in the molecular structure. The $\vec{\nu}$ vector bisects the two methyl groups and lies in the C_γ-$C_{\delta1}$-$C_{\delta2}$ plane. The angle between $\vec{\nu}$ and the methyl groups is α, the angle between the two methyl groups is, therefore, 2α. The orientation of the terminal isopropyl group can then be described by a set of Euler angles and α. As shown in Fig. 1*B*, the tilt angle θ is defined between the surface normal and $\vec{\nu}$, the twist angle η describes the rotation of the molecule with respect to $\vec{\nu}$ and ζ is the azimuthal angle of $\vec{\nu}$ in the xy-plane. Details of the model used for the qualitative analysis are summarized in the *SI Text* and in ref. 46.

^{2}H NMR Dynamic Line Shapes. To simulate the experimental ^{2}H NMR line shapes observed for selectively deuterated LKα14 peptides adsorbed onto PS, we must consider the detailed nature of leucine side chain motions. There are nine possible conformations corresponding to three rotational isomers each for the C_α-C_β and C_β-C_γ bonds. In the absence of any other motions of the side chain, four of these conformations are structurally unique (47). Models for the motion of leucine side chains are usually based on the assumption that exchange occurs between a subset of these bond rotational isomers. For example, in a ^{2}H NMR study of helical collagen fibrils with L-leucine-$^2H_{10}$ uniformly incorporated, Batchelder et al. (30) assumed exchange of the side chain between two conformers observed to be dominant in leucyl-peptide crystal structures: tg^+ and g^-t, where g^+, g^-, and t correspond to the gauche +, gauche −, and trans rotational isomers of the C_α-C_β and C_β-C_γ bonds. The temperature variation of the ^{2}H line shape was modeled as variation in the rate of exchange between these two conformations of the leucine side chain, assumed to occur with equal a priori populations.

In a ^{2}H NMR study of the transmembrane protein phospholamban in phospholipid bilayers, Lorigan and coworkers (32) modeled the ^{2}H NMR spectrum of selectively methyl-deuterated leucine as arising from the rotational motion of the methyl group, and from a two-site movement around the C_β-C_γ bond axis in which the methyl groups were tilted by 75° and jumped by 109.5°. Experimental line shapes were closely simulated with this model assuming exchange between side chain conformers with a rate constant of $k = 1 \times 10^5$ s^{-1}. A recent study of methyl-deuterated side chain

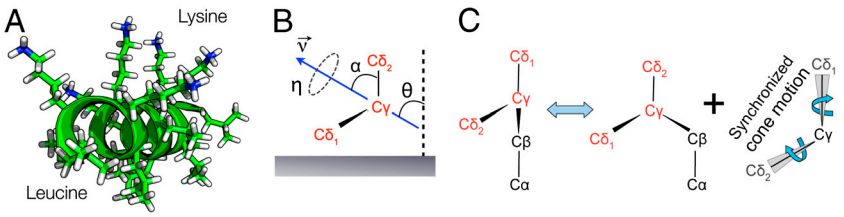

Fig. 1. (*A*) Scheme of LKα14 helical structure. (*B*) Coordinate systems used in the SFG study to quantify leucine side orientation on polystyrene. (*C*) Dynamic model for leucine side chain motions used in the ^{2}H NMR line shape study.

motions in the villin headpiece domain HP-36 by Vugmeyster et al. (47) assumed exchange between all four unique side chain conformers, with additional modulation of the ^{2}H line shape attributed to diffusion on the arc of a cone of half angle 70.5°.

The dynamic model we adopted and show in Fig. 1*C*, similar to the model of Batchelder above, assumes the side chain of leucine in a surface-adsorbed protein similarly exchanges between two configurations of the side chain: g^+t and g^-t. The overall effect of this exchange is to change the orientation of the C_γ-$C_{\delta 1}$ and C_γ-$C_{\delta 2}$ bonds by about 109.5°. The model presented in Fig. 1*C* differs from that used by Batchelder in that the a priori populations of the side chain conformers are not assumed to be equal.

The theory of the dynamically modulated solid-state ^{2}H NMR line shape is well documented (48) and discussed more fully in *SI Text*. Of interest here is the effect on the line shape of the kinetic constants k_{12} and k_{21}, representing the forward and reverse exchange between the two conformations. The kinetic constants are related to the a priori site populations by $p_1 = k_{21}/(k_{12}+k_{21})$ and $p_2 = 1 - p_1 = k_{12}/(k_{12}+k_{21})$. Because CD_3 group rotation occurs on a time scale much faster than that of configurational changes of the leucine side chain, the effect of methyl rotation can be accounted for by scaling the quadrupolar coupling constant. Additional motions at time scales comparable to or slower than the configurational change can be incorporated and calculated numerically using MXET1 (49, 50).

Methods and Materials

Details of peptide synthesis, substrate preparation, peptide-substrate binding, NMR, and SFG spectroscopic parameters are included in *SI Text*. Briefly, LKα14 peptides, Ac-LKKLLKLLKKLLKL-OH, were synthesized de novo with isopropyl-d_7 side chains at single leucine sites, abbreviated as Leu# where # is the position of the deuterated residue. Aqueous solutions of peptide were used to place monolayers on polystyrene-coated CaF_2 prisms for SFG spectroscopy, and 1.0 μm diameter polystyrene beads for NMR experiments.

Deuterium line shape simulations were obtained with a combination of the MXET1 simulation program and locally written Matlab code. The rapidly rotating $C_\delta D_3$ methyl groups were preaveraged and treated as a single superspin, with the effective quadrupolar coupling (QCC_{eff}) as an adjustable parameter. To approximate the backbone mobility of the peptide, a cone motion using the method of Vold and coworkers (47) was added to the C_α-C_β bond, consisting of a ten-site jump evenly distributed around the surface of a cone defined by a variable half angle along both the C_γ-$C_{\delta 1}$ and C_γ-$C_{\delta 2}$ bonds operating in lockstep, so that the overall $C_{\delta 1}$-C_γ-$C_{\delta 2}$ bond angle remained constant (Fig. 1*B*). A uniform rate constant of 600 s^{-1} between adjacent sites on the cone was applied in all simulations. The exchange between the two primary conformers was modeled as a global exchange rate (k_{ex}) of 6×10^6 s^{-1} for all residues (determined empirically) with a varying, site-dependent initial conformation population ratio (p_1/p_2).

Results

Sum Frequency Generation. SFG vibrational spectra in the C-D stretching range (2,000–2,300 cm^{-1}) were acquired for the series of selectively deuterated LKα14 peptides. Spectra obtained with *ssp*, *ppp*, and *sps* polarization combinations are shown in Fig. 2. Note that while peptides were also present in the surrounding buffer solution during the measurements, the spectra are only representative of ordered adsorbed peptides on the surface because of the interface specificity and selection rules of the SFG technique (17). The leucine sites in the original peptide sequence (see Fig. 1) are also indicated. The resonance positions and oscillator strengths A for the samples were obtained by fitting [**2**] to the data (*red lines* in Fig. 2). Resonances near 2,220 cm^{-1} and 2,260 cm^{-1} can be assigned to asymmetric (r^-) and symmetric (r^+) CD_3 stretching modes. Features near 2,130 cm^{-1} and 2,080 cm^{-1} are related to the CD_3 Fermi resonance (r^+_{FR}) and the CD stretching mode of the γ-carbon in the isopropyl group, respectively (51, 52). A weak additional peak observed in the *ppp* spectra near 2,150 cm^{-1} is most likely explained by a Fermi resonance of the CD moiety (53, 54). The peak intensities vary significantly for the three polarization combinations. In the *sps* spectra, only the asymmetric CD_3 mode is visible. The *ppp* spectra are also dominated by the r^- resonance, but the r^+, r^+_{FR}, and CD resonances also exhibit significant intensity. The latter modes are the most prominent features in the *ssp* spectra and the asymmetric stretching mode is much weaker. Interestingly, the phase (observed as the peak polarity and shape) of the r^- modes in the *sps* and *ppp* spectra exhibit a strong dependence on the Leu position, while the phases of the other modes are mostly unaffected. Pronounced phase variability of the r^- modes versus the r^+ modes has also been observed before in phase studies of methyl stretching modes in peptide spectra and polystyrene (55, 56). The intensities of all observed modes vary significantly with the leucine positions. Some leucines have very strong features for particular polarization combinations but only medium or low intensity in others. For example, in the *ppp* spectra, the r^- peak (2,220 cm^{-1}) is by far the strongest in the spectrum for Leu12 while all other leucines have similar

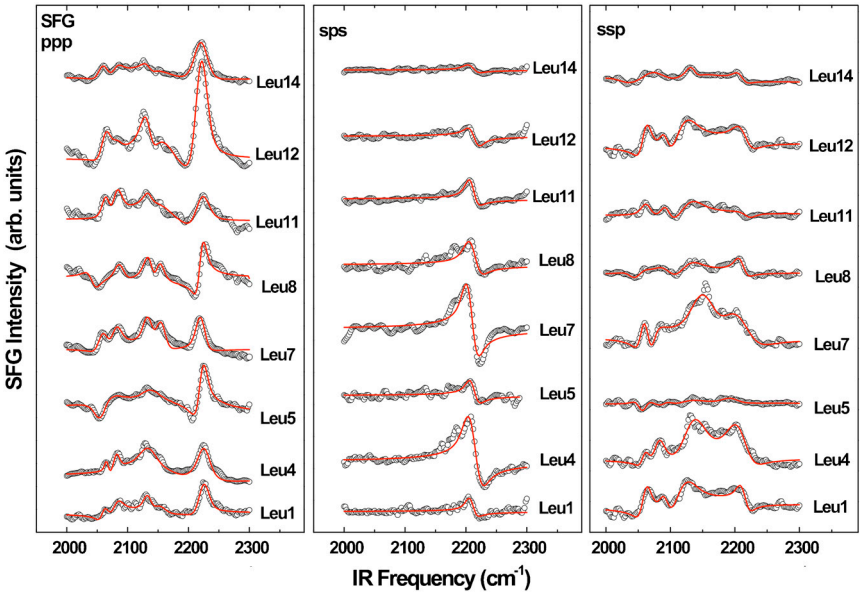

Fig. 2. *ppp*, *sps* and *ssp* SFG experimental spectra (*open circles*) and calculated fits (*red lines*) for LKα14 deuterated at each of the eight leucine sites in the peptide.

intensity levels. At the same time, Leu12 is almost featureless for *sps* and only of moderate strength for *ssp*. Conversely, Leu7 and Leu4 show the strongest r^- intensities in both *ssp* and *sps* spectra but only average intensities for *ppp*. It is interesting to note, that the overall signal intensity is not generally lower for leucines at the ends of the peptide strand. This observation shows that the side chain ordering at the center and ends of the peptide is similar since the SFG signal strongly depends on the orientational order of the respective surface species.

The side chain orientation results from a quantitative analysis of the SFG spectra, obtained as described in *Procedures*, are shown in Table 1. Two sets of intensity ratios were employed in the calculations: the ratios for the symmetric stretching modes (r^+) in the *ppp* and *ssp* spectra and the ratios for the asymmetric modes (r^-) in the *ppp* and *sps* spectra. Table 1 displays the obtained tilt and twist angles of the terminal isopropyl group along with the experimental intensity ratios. The obtained tilt angles for the adsorbed LK peptides give a detailed picture of the conformation of adsorbed LK peptides. Leucines at sites Leu1, Leu5, Leu12, and Leu14 all have tilt angles ≥68° and are bent away from the surface. The side chains Leu4, Leu7, Leu8, and Leu11, on the other hand, have tilt angles from 30° to 50° and are more oriented towards the interface and are more likely engaged in surface binding. The high-tilt side chains ($\theta \geq 68°$) show torsion angles η above 40°, while the less tilted leucines also tend to have lower torsion angles ($\eta < 30°$). The only exception is Leu8, which has a low tilt angle in combination with a higher torsion angle ($\theta \approx 48°$ and $\eta \approx 52°$), likely due to steric hindrance within the peptide chain. The strong correlation of leucine tilt and twist angles ($R^2 = 0.91$) is shown in Fig. 3. This correlation shows that as the leucines interact more strongly with the surface and the side-chain terminal methyl groups become closer to the surface, the isopropyl units tend to rotate and bring one of the methyl groups closer to the surface.

The SFG tilt angle analysis itself does not directly provide the pointing direction of the side chains. In principle, the chains could be oriented towards or away from the interface with the determined angles. In a recent combined NMR and phase sensitive SFG study the majority of leucine side chains in LK peptides on polystyrene were determined to be oriented towards the surface (41). However, individual leucines could still orient differently. Comparison of SFG-determined angles with complementary NMR side-chain dynamics data described in the following section provides a more complete picture of the peptide structure.

Solid-State NMR. The relatively narrow line shapes obtained for surface-bound peptides (black lines in Fig. 4), all approximately 37 kHz wide, indicate that the methyl groups predominate. The C_γ deuteron, with a much wider (~120 kHz) doublet pattern, contributed a mean of only 9% to the overall integration of any line shape, and in several it barely exceeded the noise level. The width also remained well within the homogeneous region of the applied RF pulses, minimizing spectral artifacts. The narrow central peak

Table 1. Tilt and twist angles of the leucine side chains obtained from SFG measurements

Deuteration position	Tilt angle/°	Twist angle/°	Ratio sym ppp/ssp	Ratio asym ppp/sps
Leu 1	70	44	1.64	3.25
Leu 4	47	27	1.70	1.58
Leu 5	68	42	1.72	2.92
Leu 7	39	21	1.52	1.58
Leu 8	48	52	1.07	3.05
Leu 11	30	17	1.17	1.47
Leu 12	82/98	45	1.72	7.69
Leu 14	74	53	1.25	5.60

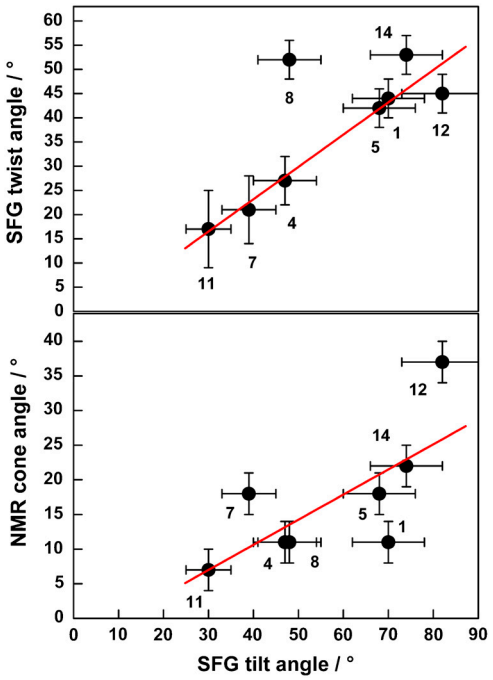

Fig. 3. *Top*: Plot of the SFG twist and tilt angles for leucines at different positions within the peptide. The linear fit (*red trace*) reveals a correlation of $R^2 = 0.96$ if Leu8 is not taken into account (0.77 including all points). *Bottom*: Correlation of SFG tilt and NMR cone angles. The correlation is weak but visible ($R^2 = 0.71$).

seen on all spectra represents trace water signal (HOD) that could not be removed completely, even by extensive lyophilization.

The backbone motion rate k_{cone} remained constant across all simulations, implying that the ends of the peptide were not significantly more mobile than the center, consistent with the SFG signal intensity results. More interesting is the angle of the cone motion, which has a weak ($R^2 = 0.71$) but visible correlation with the SFG-derived tilt angle. The cone angle is used as an approximation for the overall motion of the backbone and the C_α-C_β side-chain bond closest to the backbone. As opposed to k_{cone}, representing only an exchange rate without a fixed geometry, the cone angle should represent a physical range of mobility. Side chains with greater contact with the polystyrene are expected to be hindered by the surface, and therefore have a narrower cone angle. This prediction is borne out by comparison to the SFG data—

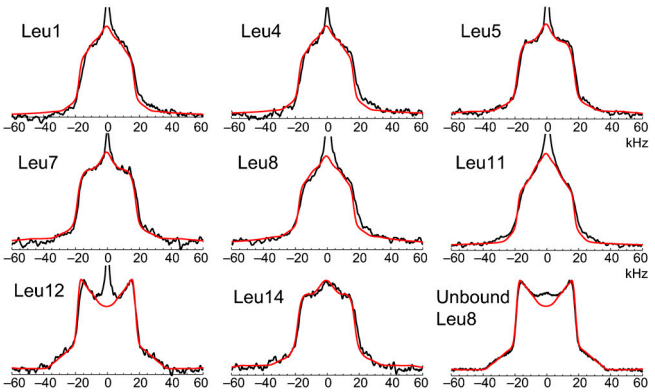

Fig. 4. Measured ssNMR line shapes (*black*) and simulated fits (*red*) for LKα14 deuterated individually at each of the eight leucine sites. The spectrum of lyophilized, unbound Leu8 is also presented for comparison (*bottom row, right*), taken under identical conditions. The simulation parameters obtained are summarized in Table 2.

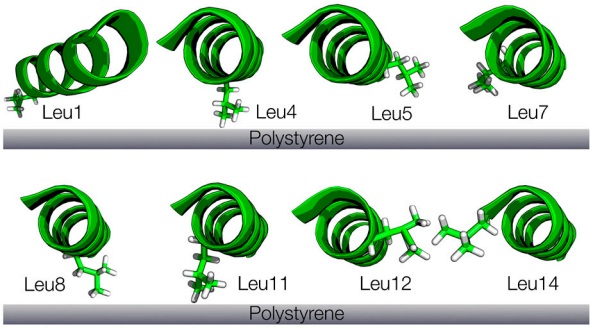

Fig. 5. Schematic drawing of the leucine orientations after adsorption based on SFG-based tilt and twist angles of the leucine isopropyl groups, NMR-determined surface vicinities and α-carbon positions estimated from the known general protein orientation and secondary structure.

Leu11 has the side chain that is closest to the surface normal, with a SFG-derived tilt angle of 30°, and correspondingly has the lowest NMR-simulated cone angle (5°). Conversely, sites that are predicted to be nearly parallel to the surface, such as Leu12 and Leu14, have high cone angles of 25° and 35°, respectively. Leu12, in particular, has a line shape clearly distinct from the other sites and a substantial difference in its conformational exchange rate, suggesting that it is the least tightly bound to the surface, borne out by the highest SFG tilt angle (82°) which is nearly parallel to the PS surface.

Discussion

Together, SFG and NMR provide a detailed, comprehensive picture of the orientations and positions of all leucine residues within LK peptides on polystyrene surfaces. Fig. 5 illustrates how tilt and torsion angles from SFG, surface proximity from NMR, and steric constraints based on the position of the residues in the peptide backbone are used to develop a surface structure model. The latter constraint, the distance of the α-carbon to the surface, can be estimated from the peptide sequence and the known orientation of the entire peptide on hydrophobic surfaces. It has been shown that the peptide assumes an α-helical secondary structure on polystyrene and that the leucine ensemble is generally oriented towards the interface while the lysines point towards the surrounding media (9, 10, 16, 41, 42).

Leu1, Leu4, Leu8, and Leu11 have α-carbons close to the surface and are probably interacting strongly with the PS surface. Side chain proximity to the surface is also reflected in low NMR cone angles of ≤11°. According to the SFG analysis, Leu4, Leu8, and Leu11 have slightly larger tilt angles (47°, 48°, and 30°, respectively) but are still oriented towards the interface and are likely also interacting with the PS surface. Leu11, the residue with the strongest tendency towards the surface (smallest tilt angle), has the lowest NMR cone angle of all leucines, likely due to its pronounced surface interactions. Conversely, Leu1 exhibits a low cone angle (11°), but is bent away from the surface. This angle means it is close to the surface, based on the position of its α-carbon in the peptide chain, but not oriented towards the interface. Leu1's position at the peptide N terminus may sterically favor a conformation where the chain points away from the peptide. In the monolayer peptide film studied here it is possible that in this orientation Leu1 could interact with hydrophobic sites of neighboring peptides.

Table 2. NMR simulation parameters for the spectra shown in Fig. 4 along with SFG-based tilt angles for comparison

Deuteration position	P1/P2	Cone angle (°)	QCC_{eff} (kHz)	γ-deuteron (%)	SFG tilt angle (°)
Leu 1	36:64	11	47	8	70
Leu 4	36:64	11	47	8	47
Leu 5	36:64	18	49	8	68
Leu 7	36:64	18	50	5	39
Leu 8	36:64	11	47	16	48
Leu 11	36:64	7	48	10	30
Leu 12	20:80	37	48	7	82
Leu 14	36:64	22	49	10	74

Leucines at sites Leu5, Leu7, Leu12, and Leu14 have their α-carbons at larger distances from the surface. The respective NMR cone angles are also significantly larger, showing more mobility and less pronounced surface interaction. In this group, Leu7 is the only residue with an orientation towards the interface ($\eta = 39°$). Leu5, Leu12, and Leu14 are bent away from the surface with tilt angles of ≥68°. Since these side chains are less involved in binding the peptide to the surface, their orientation is likely more determined by molecular interactions within the peptide. Among the high-tilt residues, the distinct NMR line shape of Leu12 deserves special consideration, since its high mobility and similarity to the line shape of the unbound peptide suggests the side chain likely has the greatest distance from the surface among all leucine residues. At the same time, its α-carbon position is not particularly distant from the surface compared to other high-tilt side chains, which can be explained by an orientation where the isopropyl group points away from the surface. SFG cannot distinguish between angles of 90° + x and 90° − x. Thus, by comparison with the other high-tilt sites the NMR results suggest that Leu12 has a likely tilt angle of 98° (i.e., pointed away from the surface).

Conclusion

This study demonstrates the power of combined SFG/NMR for obtaining structural information about peptides adsorbed onto surfaces with unprecedented resolution and detail. The orientations of all eight leucine side chains within LKα14 adsorbed onto PS were detected with SFG vibrational spectroscopy. The leucine side chain mobilities were probed with ssNMR. The results show that residues in the center of the peptide with α-carbon positions near the PS surface interact more strongly with the PS surface. In contrast, those residues at the ends of the peptide with α-carbons further away from the PS surface don't interact as strongly with the PS surface. This investigation with the model LKα14 peptides adsorbed onto PS lays the groundwork for a unique strategy to analyze more complex proteins adsorbed onto surfaces. This study underlines the importance of using complementary surface analytical tools and biochemical methods for providing a more comprehensive and molecular level understanding of adsorbed peptides, and also suggests a possible path forward for obtaining high resolution structural and dynamic information about surface-bound proteins using joint ssNMR and SFG methods.

ACKNOWLEDGMENTS. We thank Sirnegada Techane for the XPS coverage analysis and Ashley Morgan for assistance with peptide synthesis. The authors acknowledge support from the National Institutes of Health (NIH) R01 GM074511, R01 DE12554, and P41 EB002027. T.W. thanks the Deutsche Forschungsgemeinschaft (DFG) for a research fellowship.

1. Healy KE (1999) Molecular engineering of materials for bioreactivity. *Curr Opin Solid St M* 4:381–387.
2. Angelova N, Hunkeler D (1999) Rationalizing the design of polymeric biomaterials. *Trends Biotechnol* 17:409–421.
3. Ratner BD, Bryant SJ (2004) Biomaterials: where we have been and where we are going. *Annu Rev Biomed Eng* 6:41–75.
4. Vasita R, Shanmugam K, Katti DS (2008) Improved biomaterials for tissue engineering applications: surface modification of polymers. *Curr Top Med Chem* 8:341–353.
5. Borkenhagen M, Clemence JF, Sigrist H, Aebischer P (1998) Three-dimensional extracellular matrix engineering in the nervous system. *J Biomed Mater Res* 40:392–400.
6. Rezania A, Healy KE (1999) Biomimetic peptide surfaces that regulate adhesion, spreading, cytoskeletal organization, and mineralization of the matrix deposited by osteoblast-like cells. *Biotechnol Progr* 15:19–32.
7. Venugopal J, Low S, Choon AT, Ramakrishna S (2008) Interaction of cells and nanofiber scaffolds in tissue engineering. *J Biomed Mater Res B* 84B:34–48.

8. Wang J, Buck SM, Chen Z (2002) Sum frequency generation vibrational spectroscopy studies on protein adsorption. *J Phys Chem B* 106:11666–11672.
9. Samuel NT (2005) *Structural characterization of adsorbed helical and beta-sheet peptides* (University of Washington, Seattle, WA).
10. Mermut O, et al. (2006) In situ adsorption studies of a 14-amino acid leucine-lysine peptide onto hydrophobic polystyrene and hydrophilic silica surfaces using quartz crystal microbalance, atomic force microscopy, and sum frequency generation vibrational spectroscopy. *J Am Chem Soc* 128:3598–3607.
11. Wang J, Chen X, Clarke ML, Chen Z (2006) Vibrational spectroscopic studies on fibrinogen adsorption at polystyrene/protein solution interfaces: hydrophobic side chain and secondary structure changes. *J Phys Chem B* 110:5017–5024.
12. York RL, et al. (2007) Influence of ionic strength on the adsorption of a model peptide on hydrophilic silica and hydrophobic polystyrene surfaces: insight from SFG vibrational spectroscopy. *J Phys Chem C* 111:8866–8871.
13. Phillips DC, et al. (2007) Side chain, chain length, and sequence effects on amphiphilic peptide adsorption at hydrophobic and hydrophilic surfaces studied by sum frequency generation vibrational spectroscopy and quartz crystal microbalance. *J Phys Chem C* 111:255–261.
14. Chen X, Wang J, Sniadecki JJ, Even MA, Chen Z (2005) Probing alpha-helical and beta-sheet structures of peptides at solid/liquid interfaces with SFG. *Langmuir* 21:2662–2664.
15. Jung SY, et al. (2003) The Vroman effect: a molecular level description of fibrinogen displacement. *J Am Chem Soc* 125:12782–12786.
16. Weidner T, et al. (2010) Assembly and structure of alpha-helical peptide films on hydrophobic fluorocarbon surfaces. *Biointerphases* 5:9–16.
17. Shen YR (1984) *The principles of nonlinear optics* (John Wiley & Sons, New York), 1 Ed.
18. Weidner T, Apte JS, Gamble LJ, Castner DG (2010) Probing the orientation and conformation of alpha-helix and beta-strand model peptides on self-assembled monolayers using sum frequency generation and NEXAFS spectroscopy. *Langmuir* 26:3433–3440.
19. Singh BR, ed. (2000) *Infrared analysis of peptides and proteins* (American Chemical Society, Washington D.C.), Vol 750.
20. Samuel NT, McCrea KR, Gamble LJ, Ward RS, Castner DG (2005) In situ sum frequency generation characterization of adsorbed alpha-helical peptides. *Abstr Pap Am Chem S* 229:U671–U671.
21. Clarke ML, Wang J, Chen Z (2005) Conformational changes of fibrinogen after adsorption. *J Phys Chem B* 109:22027–22035.
22. Igumenova TI, et al. (2004) Assignments of carbon NMR resonances for microcrystalline ubiquitin. *J Am Chem Soc* 126:6720–6727.
23. van Rossum BJ, Castellani F, Rehbein K, Pauli J, Oschkinat H (2001) Assignment of the nonexchanging protons of the alpha-spectrin SH3 domain by two- and three-dimensional H-1-C-13 solid-state magic-angle spinning NMR and comparison of solution and solid-state proton chemical shifts. *Chembiochem* 2:906–914.
24. Gibson JM, Raghunathan V, Popham JM, Stayton PS, Drobny GP (2005) A REDOR NMR study of a phosphorylated statherin fragment bound to hydroxyapatite crystals. *J Am Chem Soc* 127:9350–9351.
25. Goobes G, et al. (2006) Folding of the C-terminal bacterial binding domain in statherin upon adsorption onto hydroxyapatite crystals. *Proc Nat'l Acad Sci USA* 103:16083–16088.
26. Raghunathan V, et al. (2006) Homonuclear and heteronuclear NMR studies of a statherin fragment bound to hydroxyapatite crystals. *J Phys Chem B* 110:9324–9332.
27. Ndao M, et al. (2009) A 13C{31P} REDOR NMR investigation of the role of glutamic acid residues in statherin- hydroxyapatite recognition. *Langmuir* 25:12136–12143.
28. Makrodimitris K, Masica DL, Kim ET, Gray JJ (2007) Structure prediction of protein-solid surface interactions reveals a molecular recognition motif of statherin for hydroxyapatite. *J Am Chem Soc* 129:13713–13722.
29. Masica DL, Gray JJ (2009) Solution- and adsorbed-state structural ensembles predicted for the statherin-hydroxyapatite system. *Biophys J* 96:3082–3091.
30. Batchelder LS, Sullivan CE, Jelinski LW, Torchia DA (1982) Characterization of leucine side-chain reorientation in collagen fibrils by solid-state 2H NMR. *Proc Nat'l Acad Sci -Bio* 79:386–389.
31. Fernandez VL, Reimer JA, Denn MM (1992) Magnetic resonance studies of polypeptides adsorbed on silica and hydroxyapatite surfaces. *J Am Chem Soc* 114:9634–9642.
32. Abu-Baker S, et al. (2007) Side chain and backbone dynamics of phospholamban in phospholipid bilayers utilizing H-2 and N-15 solid-state NMR spectroscopy. *Biochemistry* 46:11695–11706.
33. Ying WW, Irvine SE, Beekman RA, Siminovitch DJ, Smith SO (2000) Deuterium NMR reveals helix packing interactions in phospholamban. *J Am Chem Soc* 122:11125–11128.
34. Long JR, Mills FD, Ganesh OK, Antharam VC, Farver RS (2010) Partitioning, dynamics, and orientation of lung surfactant peptide KL4 in phospholipid bilayers. *BBA-Biomembranes* 1798:216–222.
35. Reif B, et al. (2006) Protein side-chain dynamics observed by solution- and solid-state NMR: comparative analysis of methyl H-2 relaxation data. *J Am Chem Soc* 128:12354–12355.
36. Agarwal V, Reif B (2008) Residual methyl protonation in perdeuterated proteins for multi-dimensional correlation experiments in MAS solid-state NMR spectroscopy. *J Magn Reson* 194:16–24.
37. Goobes G, et al. (2006) A REDOR study of diammonium hydrogen phosphate: a model for distance measurements from adsorbed molecules to surfaces. *Solid State Nucl Mag* 29:242–250.
38. Shaw WJ, Ferris K, Tarasevich B, Larson JL (2008) The structure and orientation of the C-terminus of LRAP. *Biophys J* 94:3247–3257.
39. DeGrado WF, Lear JD (1985) Induction of peptide conformation at apolar water interfaces. 1. A study with model peptides of defined hydrophobic periodicity. *J Am Chem Soc* 107:7684–7689.
40. Long JR, Oyler N, Drobny GP, Stayton PS (2002) Assembly of alpha-helical peptide coatings on hydrophobic surfaces. *J Am Chem Soc* 124:6297–6303.
41. Breen NF, Weidner T, Li K, Castner DG, Drobny GP (2009) A solid-state deuterium NMR and sum frequency generation study of the side chain dynamics of peptides adsorbed onto surfaces. *J Am Chem Soc* 131:14148–14149.
42. Weidner T, Breen NF, Drobny GP, Castner DG (2009) Amide or amine: determining the origin of the 3,300 cm^{-1} NH mode in protein SFG spectra using ^{15}N isotope labels. *J Phys Chem B* 113:15423–15426.
43. Apte JS, Collier G, Latour RA, Gamble LJ, Castner DG (2009) XPS and ToF-SIMS investigation of α-helical and β-strand peptide adsorption onto SAMs. *Langmuir* 26:3423–3432.
44. Bain CD, Davies PB, Ong TH, Ward RN, Brown MA (1991) Quantitative-analysis of monolayer composition by sum frequency vibrational spectroscopy. *Langmuir* 7:1563–1566.
45. Zhuang X, Miranda PB, Kim D, Shen YR (1999) Mapping molecular orientation and conformation at interfaces by surface nonlinear optics. *Phys Rev B* 59:12632–12640.
46. Kataoka S, Cremer PS (2006) Probing molecular structure at interfaces for comparison with bulk solution behavior: water/2-propanol mixtures monitored by vibrational sum frequency spectroscopy. *J Am Chem Soc* 128:5516–5522.
47. Vugmeyster L, et al. (2009) Probing the dynamics of a protein hydrophobic core by deuteron solid-state nuclear magnetic resonance spectroscopy. *J Am Chem Soc* 131:13651–13658.
48. Torchia DA, Szabo A (1982) Spin-lattice relaxation in solids. *J Magn Reson* 49:107–121.
49. Greenfield MS, et al. (1987) Deuterium quadrupole-echo NMR-spectroscopy. 3. Practical aspects of line shape calculations for multiaxis rotational processes. *J Magn Reson* 72:89–107.
50. Vold RL, Vold RR (1991) Deuterium relaxation in molecular solids. *Advances in Magnetic and Optical Resonance*, ed W Warren (Academic Press, San Diego), Vol 16, pp 85–171.
51. Yang CSC, Richter LJ, Stephenson JC, Briggman KA (2002) In situ vibrational resonant sum frequency spectroscopic study of the self-assembly of dioctadecyl disulfide on gold. *Langmuir* 18:7549–7556.
52. Nyquist RA (2001) *Interpreting infrared, Raman, and nuclear magnetic resonance spectra* (Academic Press, London).
53. Polavarapu PL, Smith HE (1988) Methine and methyl stretching vibrations in substituted phenylethanes. *J Phys Chem-US* 92:1774–1777.
54. Kinnaman CS, Cremeens ME, Romesberg FE, Corcelli SA (2006) Infrared line shape of an r-Carbon deuterium-labeled amino acid. *J Am Chem Soc* 128:13334–13335.
55. Lambert AG, Neivandt DJ, Briggs AM, Usadi EW, Davies PB (2002) Interference effects in sum frequency spectra from monolayers on composite dielectric/metal substrates. *J Phys Chem B* 106:5461–5469.
56. McGall SJ, Davies PB, Neivandt DJ (2004) Interference effects in sum frequency vibrational spectra of thin polymer films: an experimental and modeling investigation. *J Phys Chem B* 108:16030–16039.